

Collective synchronization as a method of learning and generalization from sparse data

Takaya Miyano*

Department of Micro System Technology, Ritsumeikan University, 1-1-1 Noji-higashi, Kusatsu, Shiga 525-8577, Japan

Takako Tsutsui†

Department of Health and Social Services, National Institute of Public Health, 2-3-6 Minami, Wako, Saitama 351-0197, Japan

(Received 10 July 2007; revised manuscript received 3 December 2007; published 21 February 2008)

We propose a method for extracting general features from multivariate data using a network of phase oscillators subject to an analogue of the Kuramoto model for collective synchronization. In this method, the natural frequencies of the oscillators are extended to vector quantities to which multivariate data are assigned. The common frequency vectors of the groups of partially synchronized oscillators are interpreted to be the template vectors representing the general features of the data set. We show that the proposed method becomes equivalent to the self-organizing map algorithm devised by Kohonen when the governing equations are linearized about their solutions of partial synchronization. As a case study to test the utility of our method, we applied it to care-needs-certification data in the Japanese public long-term care insurance program, and found major general patterns in the health status of the elderly needing nursing care.

DOI: [10.1103/PhysRevE.77.026112](https://doi.org/10.1103/PhysRevE.77.026112)

PACS number(s): 89.90.+n, 05.45.Xt, 89.20.-a

I. INTRODUCTION

Because of rapid advances in computer and information sciences over the past half century, we are seeing the burgeoning of a society that can store and accumulate diverse categories of information in databases as digital data, allowing us to access them on demand via a network-based information infrastructure. The spread of the Internet has accelerated the growth of this information society. In recent years, moreover, the concept of a “sensor network” has been proposed whereby sensor systems having wireless communication functions are deployed in the environment as an information infrastructure that enables us to remotely collect environmental data. Information accessible by networked electronic systems is growing dramatically not only in scale but in the number of categories.

An important use of such large-scale databases is to find, from a large volume of data, patterns that represent general features of the system from which the data are generated. A variety of data mining algorithms have been developed to meet such social needs. Among others, the self-organizing map (SOM) algorithm, one of the three major prototypes of artificial neural networks, devised by Kohonen with his inspiration based on neurophysiological facts on the topographical organization of the cerebral cortex, is a powerful method applicable to multivariate data [1,2]. In fact, the SOM algorithm has been in widespread use for data mining. However, the SOM algorithm as well as other existing algorithms have a bottleneck that they require prior knowledge on the general features of data to achieve feature extraction from that data. For instance, the SOM algorithm requires reference vectors at the initial stage of learning. Even if the reference vectors are generated by random selection from data, the number of reference vectors has to be determined

by some rule to initiate the learning process. In many cases, such prior information, if any, is obtained from outside the data to be analyzed, not from the data itself.

Recently, we have proposed a method for spontaneously generating features from data with multiple degrees of freedom without the use of prior knowledge about the features to be extracted [3]. Our method is based on collective synchronization in a network of coupled phase oscillators subject to an analogue of Kuramoto’s dynamics [4–7]. We substitute the phase oscillators for multivariate data whose general features we are interested in. This can be performed by assigning the multivariate data to the natural frequencies of the oscillators. In this way, each oscillator carries the data in its inherent rhythm and interacts with other oscillators whose rhythms are close to it. This dynamical process achieves spontaneous self-organization of the data, in other words, “phase transition” in the data set, through collective synchronization of the phase oscillators. The common frequency vectors of the groups of partially synchronized oscillators are interpreted to represent the general features of the data set. This method may be described as data synchronization. However, it is different from recently developed algorithms that utilize synchronization between a model and data to evaluate the appropriateness of the model approximating the dynamics underlying that data [8–10]. Although data synchronization generates the general features of data in a self-organized manner, its underlying dynamics is seemingly different from that of the SOM algorithm. As will be shown in this paper, however, it turns out that the governing equations for data synchronization become equivalent to the competitive learning rule for SOM when linearized about their partially phase-locked state. In this respect, the SOM algorithm can be viewed as a linear version of data synchronization. Thus, the reference vectors used to initiate the SOM process can be spontaneously generated during the nonlinear regime of the dynamics of the learning.

In this paper, we discuss the linkage of data synchronization to the SOM algorithm. To illustrate our viewpoint, we also introduce equations governing data synchronization that

*tmiyano@se.ritsumei.ac.jp

†tsutsui@niph.go.jp

are of a different type from those introduced in [3]. The proposed dynamics may be useful when the closeness between data vectors is measured using a nonuniform metric because a particular entry of the vectors, i.e., a particular degree of freedom of the multivariate data, is more important than the remaining entries (degrees of freedom). This paper is organized as follows. In Sec. II, we survey the central ideas of the SOM algorithm and its learning rule as a preliminary to the subsequent section. In Sec. III, we introduce the governing equations for data synchronization. Following the analysis of the dynamical nature of the governing equations, we show how the equations yield the competitive learning rule for SOM. When viewing data synchronization as a method for learning features from sparse data, it is important to assess the generality of the extracted features. In this regard, an algorithm to test for the generality of feature vectors is proposed at the end of Sec. III. This algorithm may also be useful for feature extraction by the SOM algorithm. Section IV is concerned with the numerical experiments performed to test the utility of our method. As a case study, we apply our method to find major aging processes from care-needs-certification data accumulated by Japan's long-term care insurance program. Sections V and VI are devoted to discussion and conclusions, respectively.

II. SELF-ORGANIZATION MAP ALGORITHM

The SOM algorithm developed by Kohonen [1,2] is a commonly used approach for extracting features from multivariate data. This method induces the spontaneous clustering of data vectors by competitive learning. The central principle of the SOM algorithm is summarized as follows. Given a set of M reference vectors with D degrees of freedom, $\vec{m}_i = (m_{i1}, \dots, m_{iD})$ with i from 1 to M , expressed as $\{\vec{m}_i\}_{i=1}^M$, and sample vectors (multivariate learning data) $\{\vec{x}_j\}_{j=1}^N$ with D degrees of freedom, we update the reference vectors by a competitive learning rule of the form

$$\vec{m}_i(t+1) = \vec{m}_i(t) + h(\rho_{i,j})[\vec{x}_j - \vec{m}_i(t)], \quad (1)$$

$$\rho_{i,j} = |\vec{x}_j - \vec{m}_i|, \quad (2)$$

where $h(\rho_{i,j})$ is a partitioning function defined as $h(\rho_{i,j}) = \kappa(t)$ if

$$\rho_{i,j} = \min_k (|\vec{x}_j - \vec{m}_k|)$$

with an adaptation gain $\kappa(t)$ [$0 < \kappa(t) < 1$] and $h(\rho_{i,j}) = 0$ otherwise. The nearest reference vector to \vec{x}_j exclusively utilizes \vec{x}_j to update itself. In this sense, the learning process is competitive. Equation (1), which is expressed as an on-line learning rule, runs for \vec{x}_j with j from 1 to N . We can rewrite Eq. (1) in the form of a continuous batch learning equation, which uses many sample vectors \vec{x}_j at a time to update the reference vectors:

$$\frac{d\vec{m}_i}{dt} = \frac{1}{N_i} \sum_{j=1}^N h(\rho_{i,j})(\vec{x}_j - \vec{m}_i), \quad (3)$$

$$= \frac{1}{N_i} \sum_{k=1}^{N_i} \kappa(t)(\vec{x}_{j(k)} - \vec{m}_i), \quad (4)$$

where N_i is the number of the nearest sample vectors, denoted as $\vec{x}_{j(k)}$ ($k=1, \dots, N_i$), to \vec{m}_i . In the limit $N \rightarrow \infty$,

$$\frac{1}{N_i} \sum_{k=1}^{N_i} \kappa(t)\vec{x}_{j(k)} \rightarrow \kappa(t)\vec{X}_i, \quad (5)$$

where \vec{X}_i is the mean vector over all sample vectors in the neighborhood of \vec{m}_i . Consequently,

$$\frac{d\vec{m}_i}{dt} = \kappa(t)(\vec{X}_i - \vec{m}_i). \quad (6)$$

Equation (6) implies that the competitive learning rule for SOM inherits the local mean-field character of the data space.

In the SOM algorithm, the initial values of the reference vectors $\vec{m}_i(0)$ are set using prior knowledge about the features to be extracted. If there is no such knowledge, random selection from the sample vectors suffices. There is, however, no rule to determine the appropriate initial number of reference vectors. Accordingly, the initial settings of the reference vectors are determined haphazardly. By applying sufficient iterations of Eq. (1) or Eq. (3) under such an initial setting, the reference vectors will converge to certain template vectors. These template vectors are expected to represent the general features of the population ensemble of the data from which the learning data are generated. In the following section, we discuss the link between the learning algorithm for SOM, i.e., Eq. (6) and the equations governing data synchronization.

III. DATA SYNCHRONIZATION

A. Governing equations and their link to the SOM algorithm

Given the sample vectors $\{\vec{x}_j\}_{j=1}^N$ with D degrees of freedom, we assign these multivariate data to the natural frequencies of the phase oscillators subject to an analogue of the Kuramoto model:

$$\frac{d\theta_{in}}{dt} = x_{in} + \frac{K}{N_i} \sum_{j=1}^N H(\tilde{d}_{i,j}) \sin(\theta_{jn} - \theta_{in}), \quad \tilde{d}_{i,j} = |\vec{x}_i - \vec{x}_j|, \quad (7)$$

$$n = 1, \dots, D,$$

where K is a positive coupling constant and θ_{in} is the n th entry of the phase vectors $\vec{\theta}_i = (\theta_{i1}, \dots, \theta_{iD})$, whose initial values are given as random numbers. The derivative of $\vec{\theta}_i$ with respect to time, denoted as $\vec{\omega}_i(t) = d\vec{\theta}_i/dt$, represents the updated value of \vec{x}_i at each instant in the time evolution. Hence, the phase vector $\vec{\theta}_i$ expresses the dynamical behavior of the phase oscillator carrying the updated data in its updated rhythm $\vec{\omega}_i$. The partitioning function H , which determines the range of mutual interaction between phase oscillators, is defined as $H(\tilde{d}_{i,j}) = 1$ if $\tilde{d}_{i,j} \leq \tilde{d}_0$ and $H(\tilde{d}_{i,j}) = 0$ otherwise.

Here, $\tilde{d}_0 = \alpha |\vec{x}_i|$ with a positive constant α and $|\vec{x}_i|$ is measured in terms of the Euclidean norm. This determines N_i neighboring vectors with which the phase vector $\vec{\theta}_i$ can interact. In this way, we can substitute the phase oscillators for the multivariate data. Each oscillator conveys the original and updated data by its natural and adaptive rhythms, respectively. This enables the self-organization of data in real physical space as well as in virtual data space.

The local mean-field character of the dynamics of Eq. (7) represents the statistical properties of the self-organized data in the limit $N \rightarrow \infty$. Denoting the local-order parameters and the local mean-field phase vectors as $\vec{r}_i = (r_{i1}, \dots, r_{iD})$ and $\vec{\psi}_i = (\psi_{i1}, \dots, \psi_{iD})$, respectively, which are valid in every local domain defined by the partitioning function H as

$$r_{in} \exp(i\psi_{in}) = \frac{1}{N_{ij=1}} \sum_{j=1}^N H(\tilde{d}_{i,j}) \exp(i\theta_{jn}), \quad (8)$$

we can rewrite Eq. (7) as

$$\frac{d\theta_{in}}{dt} = x_{in} + Kr_{in} \sin(\psi_{in} - \theta_{in}). \quad (9)$$

Here, we consider the phase vectors belonging to the g th group of G partially synchronized groups. The phase oscillators belonging to the same group are synchronized with each other, but they drift to those belonging to different groups. Let us denote each entry of a phase vector belonging to the g th group as $\theta_{i(g)n} = \psi_{gn} + \Delta\theta_{i(g)n}$ and its common frequency as $X_{gn} = d\psi_{gn}/dt$, where $\vec{X}_g = (X_{g1}, \dots, X_{gD})$ with g from 1 to G . Then, Eq. (9) becomes

$$\frac{d\Delta\theta_{i(g)n}}{dt} = x_{i(g)n} - X_{gn} + Kr_{gn} \sin(\Delta\theta_{i(g)n}). \quad (10)$$

This equation implies that the frequency vector will converge to the true mean frequency vector in the partially synchronized group in the limit $N \rightarrow \infty$. In this way, partial phase lockings of the oscillators are achieved and the multivariate data undergo spontaneous grouping. The common frequency vectors \vec{X}_g are interpreted as the template vectors that represent the general features of the learning data.

The necessary condition for the setting of K to achieve partial synchronization can be derived from Eq. (10) by considering its fixed point. That is, $Kr_{in} \geq |x_{in} - X_{gn}|$. Thus, K is set to a sufficiently large value to satisfy this condition. α is determined so as to yield a sufficient number of neighbors in the neighborhood of \vec{x}_i . The size of the neighborhood in which the phase vector associated with \vec{x}_i can interact with its neighboring vectors is determined by α . In fact, the vertical angle ϕ between \vec{x}_i and its outermost neighbor is defined as $\phi = \sin^{-1}(\tilde{d}_0/|\vec{x}_i|) = \sin^{-1}\alpha$. For instance, $\phi \approx 18^\circ, 44^\circ$, and 64° when $\alpha = 0.3, 0.7$, and 0.9 , and $\phi = 30^\circ$ when $\alpha = 0.5$, respectively. In this context, α represents the coarse-graining level in data clustering. Thus, we can control the resolution for discriminating one partially synchronized group from another by adjusting the value of α .

To establish the link between data synchronization and the SOM algorithm, let us return to Eq. (9) and consider the time

evolution in the g th group, denoted as Γ_g , of the phase oscillators,

$$\begin{aligned} \omega_{in} &= x_{in} + Kr_{gn} \sin(\psi_{gn} - \theta_{in}), \\ \omega_{in} &= \frac{d\theta_{in}}{dt}, \end{aligned} \quad (11)$$

where $i \in \Gamma_g$. Equation (11) is linearized about $\psi_{gn} - \theta_{in} = 0$, i.e., the partially synchronized state:

$$\omega_{in} \approx x_{in} + Kr_{gn}(\psi_{gn} - \theta_{in}). \quad (12)$$

Taking the derivative of both sides of Eq. (12) with respect to time, we obtain

$$\frac{d\omega_{in}}{dt} = Kr_{gn}(\Omega_{gn} - \omega_{in}). \quad (13)$$

Here, \vec{r}_g are assumed to change slowly with time and be constant near $\psi_{gn} - \theta_{in} = 0$, and $\vec{\Omega}_g = d\vec{\psi}_g/dt$. By the substitutions of

$$\vec{\omega}_i = \vec{m}_i,$$

$$Kr_{gn} = \kappa(t) = \kappa = \text{const},$$

$$\vec{\Omega}_g = \vec{X}_g,$$

we can reproduce Eq. (3) from Eq. (13), since $\vec{\Omega}_g$ should approach \vec{X}_g as the number of sample vectors increases by setting an appropriate value of α , which determines the size of Γ_g . This indicates that the competitive learning rule for SOM can be derived from the linearization of the dynamics for data synchronization about its partially synchronized state.

We next introduce a different version of dynamics for data synchronization that can yield the SOM algorithm with a time-dependent coefficient $\kappa(t)$:

$$\frac{d\theta_{in}}{dt} = x_{in} + \frac{K}{N_{ij=1}} \sum_{j=1}^N (\theta_{jn} - \theta_{in}) H(\tilde{d}_{i,j}) \sin(\beta s_{i,j}), \quad (14)$$

$$s_{i,j} = \|\vec{\theta}_i - \vec{\theta}_j\|_w, \quad (15)$$

$$\tilde{d}_{i,j} = \|\vec{x}_i - \vec{x}_j\|_w. \quad (16)$$

Here, the mutual interaction is defined as a function of the distance between phase vectors, $s_{i,j}$, with a positive constant β . The dynamics of Eq. (14) is useful when $s_{i,j}$ as well as $\tilde{d}_{i,j}$ are defined as a weighted norm of the general form:

$$s_{i,j} = \sqrt{\sum_{n=1}^D w_n (\theta_{in} - \theta_{jn})(\theta_{in} - \theta_{jn})}, \quad (17)$$

$$\tilde{d}_{i,j} = \sqrt{\sum_{n=1}^D w_n (x_{in} - x_{jn})(x_{in} - x_{jn})}, \quad (18)$$

where w_n with n from 1 to D are the positive diagonal terms of a diagonal matrix that represents the metric of the phase

space. When a particular entry of a vector, for instance the k th entry, is more important than the other entries, $w_k > w_n$ for $k \neq n$. The dynamics of Eq. (14) does not inherit the mean-field character of the Kuramoto model. In this sense, the dynamics of Eq. (14) is qualitatively different from that of Eq. (7). However, an interesting application of Eq. (14) may be collective synchronization under a time-dependent metric with $w_n = w_n(t)$, which can model synchronous behavior in a version of evolving networks. In this work, we use a uniform metric with $w_n = 1$ for all n for simplicity, which has been assumed for Eq. (7).

Let us introduce the variables $z = \theta_{jm} - \theta_{im}$ and $\epsilon = \sum_{n \neq m} (\theta_{jn} - \theta_{in})^2$. Then, Eq. (14) can be rewritten as

$$\frac{d\theta_{im}}{dt} = x_{im} + \frac{K}{N} \sum_{j=1}^N z H(\tilde{d}_{i,j}) \sin(\beta \sqrt{z^2 + \epsilon}). \quad (19)$$

Furthermore, using $\Delta z = \Delta \theta_{jm} - \Delta \theta_{i(g)m}$ and $\Delta \epsilon = \sum_{n \neq m} (\Delta \theta_{jn} - \Delta \theta_{i(g)n})^2$ on the assumptions that $\tilde{\theta}_{i(g)} = \tilde{\psi}_g + \Delta \tilde{\theta}_{i(g)}$ and $\tilde{\theta}_j = \tilde{\psi}_g + \Delta \tilde{\theta}_j$, Eq. (19) is expressed for the phase vectors belonging to the g th partially synchronized group as follows:

$$\frac{d\Delta \theta_{i(g)m}}{dt} = (x_{i(g)m} - X_{gm}) + \frac{K}{N} \sum_{j=1}^N \Delta z H(\tilde{d}_{i,j}) \sin(\beta \sqrt{\Delta z^2 + \Delta \epsilon}). \quad (20)$$

Equation (20) implies that the mutual interaction weakens rapidly as $\Delta z \rightarrow 0$ and induces a slow time evolution compared with that resulting from Eq. (10). Equation (14), however, does not appear to maintain the local mean-field character. In this regard, its dynamical properties seem to differ from those of Eq. (7). Nevertheless, when we consider the sinusoidal term on the right-hand side of Eq. (14) as a time-dependent parameter that decreases monotonically to zero as $s_{i,j} \rightarrow 0$ and the dynamical process progresses toward the partial phase-locking state, Eq. (14) practically becomes a variant of Eq. (7) for small values of $|\theta_{jm} - \theta_{im}|$ with a time-dependent monotonically decreasing coupling constant $K = K(t)$

$$\frac{d\theta_{im}}{dt} = x_{im} + \frac{1}{N} \sum_{j=1}^N K(t) H(\tilde{d}_{i,j}) (\theta_{jm} - \theta_{im}). \quad (21)$$

Hence data synchronization should be also achieved by Eq. (20), and its rate of convergence to a synchronized state will be slower than that achieved by Eq. (7).

These observations lead to the derivation of the SOM algorithm with a time-dependent coefficient $\kappa(t)$. To see this, we rewrite Eq. (14) as

$$\omega_{in} = x_{in} + \frac{K}{N} \sum_{j=1}^N (\theta_{jn} - \theta_{in}) H(\tilde{d}_{i,j}) \sin(\beta s_{i,j}). \quad (22)$$

Linearization of the right-hand side of Eq. (22) about $\theta_{jn} - \theta_{in} = 0$ leads to

$$\omega_{in} \approx x_{in} + \frac{K}{N} \sum_{j \in \Gamma_g} (\theta_{jn} - \theta_{in}) H(\tilde{d}_{i,j}) \sin(\beta \sqrt{\epsilon}). \quad (23)$$

Taking the derivative of both sides of Eq. (23) with respect to time, we obtain

$$\frac{d\omega_{in}}{dt} = \frac{1}{N} \sum_{j \in \Gamma_g} \kappa(t) (\omega_{jn} - \omega_{in}), \quad (24)$$

$$\kappa(t) = KH(\tilde{d}_{i,j}) \sin(\beta \sqrt{\epsilon}). \quad (25)$$

Here, we assume that ϵ decreases slowly with time near the synchronized state, which is likely to be true. Since $\kappa(t)$ is a monotonically decreasing parameter with time and

$$\frac{1}{N} \sum_{j \in \Gamma_g} \tilde{\omega}_j \rightarrow \tilde{X}_g, \quad (26)$$

Eq. (24) becomes equivalent to Eq. (6).

The above analysis implies that data synchronization includes the SOM algorithm as its linearized version. The initial settings of the reference vectors for the SOM algorithm are spontaneously determined during the nonlinear regime of data synchronization.

In applying Eq. (7) or Eq. (14) to actual data, it is convenient to measure the degree of synchrony of the oscillators by the mean diversity σ defined below:

$$\sigma = \frac{1}{N} \sum_{i=1}^N \sigma_i = \frac{1}{N} \sum_{i=1}^N \left[\frac{1}{N} \sum_{j=1}^N H(\tilde{d}_{i,j}) \frac{d_{i,j}}{\tilde{d}_0} \right], \quad (27)$$

$$d_{i,j} = |\dot{\theta}_i - \dot{\theta}_j|. \quad (28)$$

In a completely synchronized state, $\sigma \rightarrow 0$. In the opposite extreme where every \tilde{x}_i initially has no neighbors within a distance of \tilde{d}_0 , the mean diversity σ will maintain a value of zero from the beginning of the synchronization process.

B. Test for the generality of feature vectors

Suppose that the dynamics of Eq. (7) or Eq. (14) generates template vectors $\{\tilde{X}_g\}_{g=1}^G$ from $\{\tilde{x}_i\}_{i=1}^N$. We may view data synchronization as a learning process to capture the general features of the population ensemble for $\{\tilde{x}_i\}_{i=1}^N$. Then, $\{\tilde{X}_g\}_{g=1}^G$ should also form major synchronous groups for another set of learning data $\{\tilde{y}_i\}_{i=1}^N$ that belong to the same population ensemble as $\{\tilde{x}_i\}_{i=1}^N$ but are other selections from that ensemble.

To test for the generality of the template vectors, we construct the following procedure. We add $\{\tilde{X}_g\}_{g=1}^G$ to $\{\tilde{y}_i\}_{i=1}^N$, and assign the combined vectors to the natural frequency vectors in the following manner:

$$\frac{d\theta_{i(g)n}}{dt} = X_{gn} + \frac{K_g}{N_{i(g)}} \sum_{j=1}^{G+N} H(\tilde{d}_{i(g),j}) \sin(\theta_{jn} - \theta_{i(g)n}), \quad (29)$$

$$\frac{d\theta_{i(k)n}}{dt} = y_{i(k)n} + \frac{K}{N_{i(k)}} \sum_{j=1}^{G+N} H(\tilde{d}_{i(k),j}) \sin(\theta_{jn} - \theta_{i(k)n}). \quad (30)$$

Here, $i(g)$ are the indexes of the phase oscillators to which $\{\vec{X}_g\}_{g=1}^G$ are assigned, $i(k)$ are those to which $\{\vec{y}_j\}_{j=1}^N$ are assigned, $j=i(g)$ or $i(k)$, and the positive coupling constant K_g is sufficiently smaller than K , i.e., $K_g \ll K$. In the extreme setting, K_g can be set to zero. Under such settings of K_g , the rhythms of the oscillators $i(g)$ do not change during the synchronization process, but they force other oscillators $i(k)$ to synchronize with one of $i(g)$. In this context, we may call $\{\vec{X}_g\}_{g=1}^G$ “stubborn” vectors. The stubborn vectors may correspond to a modified version of the reference vectors for the SOM algorithm, although they are not updated during the synchronization (learning) process.

We can evaluate the generality of $\{\vec{X}_g\}_{g=1}^G$ by observing how many sample vectors of $\{\vec{y}_j\}_{j=1}^N$ synchronize with the stubborn vectors. If many oscillators conveying $\{\vec{y}_j\}$ synchronize with the oscillator conveying \vec{X}_g , we can accept that \vec{X}_g captures a general feature of the population ensemble of the learning data. Otherwise, it may reflect an idiosyncratic feature of the particular learning data $\{\vec{x}_j\}_{j=1}^N$.

IV. NUMERICAL EXPERIMENTS

We performed a numerical experiment using the two types of dynamics represented by Eqs. (7) and (14). The multivariate data used in this experiment were the same as those used in [3], where three major patterns of the aging process were generated from the data and are reproduced as classes 1a, 2a, and 3a in Table I. The data were a random selection from the care-needs-certification data accumulated by Japan’s long-term care insurance program, which was launched in 2000 [11–13]. A brief description of the data is given below. In this insurance program, an elderly person aged 65 years or older in need of care is certified as belonging to a particular care class on the basis of his or her physical and mental health status [14]. At the time of certification, the user undergoes an 85-item survey on his or her physical and mental health status. The results of this survey are assessed using an electronic system, and a judgment as to the person’s care class is given using 73 of these 85 survey items [11]. A final decision on the care class is made by a care-needs-certification committee composed of experienced professionals based on the above assessment, on a general survey conducted by the user’s examiner, and on a brief submitted by a medical practitioner. Survey items and possible scores for each item are listed in the first two columns on the left in Tables I and II.

Since the launch of Japan’s long-term care insurance program, certification data for the entire country have accumulated in a database as multivariate data consisting of scores for 73 survey items and assessed care classes. The amount of data collected has reached about 25 million cases [11], which is a huge volume of data reflecting the health status of elderly persons needing nursing care in Japan. If common feature patterns were to be discovered among the many elderly

persons needing nursing care, that information would be valuable in preparing future revisions of the insurance program. However, samples of replies to the survey items constitute multivariate data with 73 degrees of freedom; thus, attempting to extract patterns using existing data mining techniques would be very difficult, if not impossible.

To assess the generality of the previous results based on Eq. (7), we performed the same experiment using Eq. (14). In this experiment, we assumed that all survey items are equally important for representing the aging process. Hence, a uniform metric $w_n=1$ for all n was used in Eq. (14). However, if particular survey items are more important than the other items for capturing the features of the aging process, which would be revealed in future works, the present experiment may provide a good benchmark for assessing the effect of a nonuniform metric on the extracted patterns.

We used 12 sets of 2000 cases comprising the same care-needs-certification data as that from which classes 1a, 2a, and 3a were extracted. We applied Eq. (14) with $K=0.4$, $\alpha=0.7$, and $\beta=\pi d_{i,j}/2\tilde{d}_0$, using a time-step width of 0.1 in the 4th-order Runge-Kutta method. The coupling constant K was determined in accordance with the necessary condition for achieving the fixed points of Eq. (14). The coarse-graining level α was selected on the basis of our recent work [15], in which the sizes and the number of major groups generated from a set of care-needs-certification data were observed as a function of α , in particular at $\alpha=0.3, 0.5, 0.7$ and 0.9 , to find the optimal value of α in terms of the medical plausibility of the extracted features.

Table I shows the major patterns extracted from the data sets, labeled as classes 1b, 2b, and 3b. The data belonging to the three patterns of classes 1b, 2b, and 3b comprise about 75% of all sample data. The three patterns of classes 1b, 2b, and 3b are essentially the same as those of classes 1a, 2a, and 3a, respectively.

Figure 1 shows the results of measuring the mean diversity σ as a function of time in the data synchronization process. The solid line represents results using Eq. (7) and the dashed line results using Eq. (14). In either case, data synchronization having an equivalent order is achieved, and as expected from the differences in dynamics, convergence is faster for Eq. (7) but slower and smoother for Eq. (14).

To examine the dependence of the extracted features on the selection of data, we next performed another numerical experiment using the dynamics of Eq. (7) together with the testing algorithm described in Sec. III B for three sets of 2000 cases of care-needs-certification data provided by Otsu City, which is a historical city contiguous to Kyoto City. In these experiments, the three feature patterns of classes 1a, 2a, and 3a were utilized as the stubborn vectors with $K_g=0$. If major feature patterns essentially equivalent to classes 1a, 2a, and 3a are reproducibly extracted from the data samples, we can be confident of the generality of the three classes.

We applied Eq. (7) with $K=10$ and $\alpha=0.7$ using a time-step width of 0.1 in the fourth-order Runge-Kutta method. The coupling constant K and the coarse-graining level α were determined in much the same way as in the first experiment using Eq. (14), as described above. Table II shows two major patterns extracted from the data samples, labeled as

TABLE I. Major patterns in the health status of elderly people needing nursing care, extracted using Eqs. (7) and (14). The first column lists the 73 items making up the care-needs-certification survey and the second column lists integer scores to be used as replies to each item. An integer score of “-1” means “healthy,” while integer scores of “1” and above indicate a health problem (a higher score represents increasing deterioration). The third to eighth columns show scores for the three major patterns obtained by data synchronization: Classes 1a, 2a, and 3a using Eq. (7) and classes 1b, 2b, and 3b using Eq. (14).

Survey item	Score	Class 1a	Class 2a	Class 3a	Class 1b	Class 2b	Class 3b
1. Paralysis (left arm)	-1,1	-0.9	-0.9	-1	-1	-0.8	-0.6
2. Paralysis (right arm)	-1,1	-0.9	-0.9	-0.9	-1	-0.9	-0.6
3. Paralysis (left leg)	-1,1	-0.2	0	0.2	-0.4	0.1	0.7
4. Paralysis (right leg)	-1,1	-0.2	-0.2	-0.4	-0.4	0	0.6
5. Paralysis (other part of body)	-1,1	-0.8	-0.8	-0.9	-0.9	-0.9	-0.8
6. Contracture (shoulder joints)	-1,1	-0.8	-0.8	-0.7	-0.9	-0.8	-0.6
7. Contracture (elbow joints)	-1,1	-0.9	-0.9	-0.8	-1	-0.9	-0.8
8. Contracture (hip joints)	-1,1	-0.8	-0.8	-0.8	-0.9	-0.9	-0.7
9. Contracture (knee joints)	-1,1	-0.3	-0.3	-0.3	-0.4	-0.3	-0.3
10. Contracture (ankle joints)	-1,1	-0.8	-0.9	-1	-0.9	-0.9	-0.8
11. Contracture (other part of body)	-1,1	-0.6	-0.6	-0.6	-0.7	-0.7	-0.6
12. Rolling over in bed	-1,1,2	-0.5	0.6	0.4	-0.7	-0.3	0.5
13. Sitting up in bed	-1,1,2	0.1	0.3	0.4	0	0.4	1
14. Sitting with both feet on floor	-1,1,2,3	-0.7	0.4	0.6	-0.8	-0.4	0.8
15. Sitting without feet on floor	-1,1,2,3	0	0.5	0.5	-0.2	0.4	1.2
16. Standing on both feet	-1,1,2	-0.8	0.3	0.5	-0.9	-0.5	1
17. Walking	-1,1,2	0.6	0.6	0.6	0.5	0.8	1.2
18. Transferring	-1,1,2,3	0.6	0.7	0.7	0.5	0.9	1.5
19. Standing up from sitting position	-1,1,2	-0.6	1.5	1	-0.7	-0.1	1.4
20. Standing on one foot	-1,1,2	-0.9	-0.9	-0.8	-1	-1	-0.9
21. Getting in and out bath	-1,1,2,3	-0.7	-0.7	-0.6	-0.8	-0.7	-0.6
22. Bathing	-1,1,2,3	-0.8	-0.8	-0.9	-0.9	-0.9	-0.5
23. Bedsore (decubitus ulcer)	-1,1	-0.9	-0.5	0.6	-1	-0.8	0
24. Other skin diseases	-1,1	-0.9	-0.1	0	-1	-0.7	0.6
25. Lifting one arm to the chest	-1,1,2	-0.9	-0.3	0.3	-1	-0.7	0.6
26. Swallowing	-1,1,2	-0.9	-0.2	1.4	-1	-0.8	0.5
27. Desire to urinate	-1,1,2	-0.3	1.8	1.3	-0.4	0.2	1.6
28. Desire to defecate	-1,1,2	-0.9	1.3	1.4	-0.9	-0.5	1.7
29. Management after urination	-1,1,2,3	-0.9	1.7	1.7	-0.9	-0.4	1.9
30. Management after defecation	-1,1,2,3	-0.7	0.1	0.6	-0.6	-0.3	1
31. Taking meals (dietary intake)	-1,1,2,3	-0.5	0.7	0.7	-0.4	-0.1	1.4
32. Oral hygiene (tooth brushing)	-1,1,2	-0.6	-0.6	-0.7	-0.7	-0.6	-0.3
33. Face washing	-1,1,2	-0.3	-0.3	-0.4	-0.3	-0.2	0.1
34. Hair care	-1,1,2	-0.9	-0.8	-0.2	-1	-0.9	-0.1
35. Nail cutting	-1,1,2	-0.9	-0.9	-1	-0.9	-0.9	-0.3
36. Buttoning and unbuttoning clothing	-1,1,2,3	-0.9	-0.7	0.1	-0.9	-0.9	0
37. Putting on and taking off a jacket	-1,1,2,3	-0.9	-0.9	-0.9	-1	-1	-0.5
38. Putting on and taking off trousers	-1,1,2,3	-0.9	-0.9	-0.4	-0.9	-0.9	-0.1
39. Putting on and taking off socks	-1,1,2,3	-0.9	-0.9	-0.8	-1	-1	-0.9
40. Cleaning rooms	-1,1,2	-0.9	-0.9	-0.8	-0.9	-0.9	-0.3
41. Taking medication	-1,1,2	-0.9	-0.9	-0.9	-1	-1	-0.5
42. Financial management	-1,1,2	-0.9	-0.9	-0.7	-0.9	-1	-0.8
43. Serious memory loss	-1,1,2	-0.9	-0.9	-0.9	-1	-1	-0.9
44. Loss of interest in circumstances	-1,1,2	-0.9	-0.9	-0.8	-1	-1	-0.8

TABLE I. (Continued.)

Survey item	Score	Class 1a	Class 2a	Class 3a	Class 1b	Class 2b	Class 3b
45. Visual acuity	-1,1,2,3,4	-0.9	-0.9	-0.8	-0.9	-0.9	-0.7
46. Hearing	-1,1,2,3,4	-0.8	-0.8	-0.8	-0.9	-0.9	-0.6
47. Mutual communication	-1,1,2,3	-0.9	-0.9	-0.8	-1	-1	-0.9
48. Response to instructions	-1,1,2	-0.8	-0.9	-0.8	-0.8	-0.9	-0.7
49. Understanding a daily schedule	-1,1	-0.9	-0.9	-0.8	-1	-1	-0.8
50. Answering date of birth and age	-1,1	-0.9	-0.9	-0.4	-1	-1	-0.5
51. Short-term memory	-1,1	-0.9	-0.9	-0.8	-1	-1	-0.7
52. Remembering own name	-1,1	-0.9	-0.9	-0.8	-1	-1	-0.9
53. Recognition of current season	-1,1	-0.9	-0.9	-0.8	-1	-1	-0.9
54. Orientation in place	-1,1	-0.9	-0.9	-0.8	-1	-1	-0.9
55. Feeling persecuted	-1,1,2	-0.9	-0.9	-0.8	-1	-1	-1
56. Fabricating stories	-1,1,2	-0.8	-0.9	-0.9	-0.9	-0.9	-1
57. Visual or auditory hallucinations	-1,1,2	-0.9	-0.9	-0.8	-1	-1	-1
58. Emotional instability	-1,1,2	-0.9	-0.9	-0.8	-1	-1	-0.8
59. Reversion of day and night	-1,1,2	-0.9	-0.9	-0.8	-1	-1	-0.9
60. Verbal or physical violence	-1,1,2	-0.4	-0.4	0.5	-0.3	-0.4	0.4
61. Repeating the same story	-1,1,2	-0.7	0.1	0.4	-0.9	-0.5	0.5
62. Shouting	-1,1,2	0	1.4	0.5	-0.1	0.3	1.2
63. Resisting advice or care	-1,1,2	-0.5	1.2	1.3	-0.6	0	1.6
64. Poriomania	-1,1,2	-0.9	-0.9	-0.9	-1	-1	-1
65. Restlessness	-1,1,2	-0.9	-0.6	0.2	-1	-0.9	-0.1
66. Being away from residence	-1,1,2	-0.9	-0.7	-0.3	-1	-0.9	-0.2
67. Insisting on going out alone	-1,1,2	-0.8	0.6	1.8	-0.9	-0.5	1.4
68. Collecting mania	-1,1,2	-0.9	0.5	1.5	-1	-0.6	1.3
69. Inability to manage a fire	-1,1,2	-0.9	1.4	1.4	-1	-0.5	1.5
70. Destruction of things or clothes	-1,1,2	-0.9	1.5	1.7	-0.9	-0.4	1.8
71. Unsanitary behavior and living conditions	-1,1,2	0.7	1	1.2	0.7	1.1	1.9
72. Pica (consumption of nonnutritive substances)	-1,1,2	-0.9	-0.9	1.4	-0.9	-0.9	-0.1
73. Troublesome sexual behavior	-1,1,2	-0.9	-0.9	-0.9	-1	-1	-1

classes 1c and 4. For the three sets of data samples, the data belonging to the patterns of classes 1c and 4 comprise about 42–43 % and 30–33 % of all sample data, respectively. Figure 2 shows the mean diversity σ as a function of time in the data synchronization process. In every data set, data synchronization with an equivalent order is achieved. It appears that class 1c is equivalent to class 1a, since the main feature of class 1c is of functionally impaired legs and hindered movement when using the legs, which is similar to that of class 1a. On the other hand, class 4 seems to correspond with none of classes 1a, 2a, and 3a. In fact, class 4 is different from class 1a in deteriorating ability at daily living and from classes 2a and 3a in ability of mental judgment at social daily living. The stubborn vectors of classes 2a and 3a fail to form major groups of synchronized oscillators. Consequently, the aging pattern of class 1 can be viewed as one of the major general aging patterns, whereas we should no longer refer to the generality of other classes within the present numerical experiments.

V. DISCUSSION

In the present work, we clarified the link between data synchronization and the SOM algorithm. Data synchronization can reproduce the competitive learning rule for SOM as its linear version when the phase oscillators approach partially synchronized states. During the nonlinear regime of the dynamics, data synchronization spontaneously determines the initial settings for the reference vectors of the SOM algorithm. We can thus find a method of fixing the problem of determining the initial settings haphazardly to initiate the learning process for SOM.

An advantage of data synchronization is the controllability of the coarse-graining level for data clustering through the adjustable parameter α . α is set to a small value to extract fine features of given data, and to a large value to capture a few global features of the data. In this work, α was set to 0.7, which yielded two or three major groups of partially synchronous oscillators. If we set α to 0.5, we can obtain

TABLE II. Major patterns in the health status of elderly people needing nursing care, extracted from three sets of 2000 cases of care-needs-certification data provided by Otsu City using Eq. (7) with stubborn vectors of classes 1a, 2a, and 3a. The third and fourth columns show scores for the two major patterns labeled as classes 1c and 4, respectively.

Survey item	Score	Class 1c	Class 4
1. Paralysis (left arm)	-1,1	-0.9	-0.4
2. Paralysis (right arm)	-1,1	-0.9	-0.7
3. Paralysis (left leg)	-1,1	-0.4	0.6
4. Paralysis (right leg)	-1,1	-0.3	0.5
5. Paralysis (other part of body)	-1,1	-0.8	-0.8
6. Contracture (shoulder joints)	-1,1	-0.8	-0.5
7. Contracture (elbow joints)	-1,1	-0.9	-0.8
8. Contracture (hip joints)	-1,1	-0.8	-0.8
9. Contracture (knee joints)	-1,1	-0.3	-0.3
10. Contracture (ankle joints)	-1,1	-0.8	-0.8
11. Contracture (other part of body)	-1,1	-0.7	-0.7
12. Rolling over in bed	-1,1,2	-0.6	0.7
13. Sitting up in bed	-1,1,2	0.1	1
14. Sitting with both feet on floor	-1,1,2,3	-0.7	1
15. Sitting without feet on floor	-1,1,2,3	0.1	1.4
16. Standing on both feet	-1,1,2	-0.7	1
17. Walking	-1,1,2	0	1.3
18. Transferring	-1,1,2,3	-0.9	1.6
19. Standing up from sitting position	-1,1,2	0.5	1.2
20. Standing on one foot	-1,1,2	0.5	1.3
21. Getting in and out bath	-1,1,2,3	-0.6	1.6
22. Bathing	-1,1,2,3	-0.7	1.4
23. Bedsore (decubitus ulcer)	-1,1	-0.9	-0.9
24. Other skin diseases	-1,1	-0.6	-0.7
25. Lifting one arm to the chest	-1,1,2	-0.9	-0.9
26. Swallowing	-1,1,2	-0.9	-0.5
27. Desire to urinate	-1,1,2	-0.9	0.2
28. Desire to defecate	-1,1,2	-0.9	0
29. Management after urination	-1,1,2,3	-0.8	1.6
30. Management after defecation	-1,1,2,3	-0.8	1.9
31. Taking meals (dietary intake)	-1,1,2,3	-0.9	0.6
32. Oral hygiene (tooth brushing)	-1,1,2	-0.9	0.8
33. Face washing	-1,1,2	-0.9	0.6
34. Hair care	-1,1,2	-0.9	0.6
35. Nail cutting	-1,1,2	-0.5	1.6
36. Buttoning and unbuttoning clothing	-1,1,2,3	-0.9	1.7
37. Putting on and taking off a jacket	-1,1,2,3	-0.9	1.9
38. Putting on and taking off trousers	-1,1,2,3	-0.9	2.1
39. Putting on and taking off socks	-1,1,2,3	-0.9	2.1
40. Cleaning rooms	-1,1,2	0.6	1.6
41. Taking medication	-1,1,2	-0.7	0.9
42. Financial management	-1,1,2	-0.5	1.2
43. Serious memory loss	-1,1,2	-0.6	-0.5
44. Loss of interest in circumstances	-1,1,2	-0.9	-0.7
45. Visual acuity	-1,1,2,3,4	-0.6	-0.3
46. Hearing	-1,1,2,3,4	-0.4	0

TABLE II. (Continued.)

Survey item	Score	Class 1c	Class 4
47. Mutual communication	-1,1,2,3	-0.9	0.1
48. Response to instructions	-1,1,2	-0.9	-0.6
49. Understanding a daily schedule	-1,1	-0.9	-0.5
50. Answering date of birth and age	-1,1	-0.9	-0.6
51. Short-term memory	-1,1	-0.9	-0.5
52. Remembering own name	-1,1	-0.9	-0.9
53. Recognition of current season	-1,1	-0.9	-0.5
54. Orientation in place	-1,1	-0.9	-0.6
55. Feeling persecuted	-1,1,2	-0.9	-0.9
56. Fabricating stories	-1,1,2	-0.9	-0.9
57. Visual or auditory hallucinations	-1,1,2	-0.9	-0.9
58. Emotional instability	-1,1,2	-0.9	-0.9
59. Reversion of day and night	-1,1,2	-0.8	-0.9
60. Verbal or physical violence	-1,1,2	-0.9	-0.9
61. Repeating the same story	-1,1,2	-0.8	-0.9
62. Shouting	-1,1,2	-0.9	-0.9
63. Resisting advice or care	-1,1,2	-0.9	-0.9
64. Poriomania	-1,1,2	-0.9	-0.9
65. Restlessness	-1,1,2	-0.9	-0.9
66. Being away from residence	-1,1,2	-0.9	-0.9
67. Insisting on going out alone	-1,1,2	-0.9	-0.9
68. Collecting mania	-1,1,2	-0.9	-0.9
69. Inability to manage a fire	-1,1,2	-0.8	-0.8
70. Destruction of things or clothes	-1,1,2	-0.9	-0.9
71. Unsanitary behavior and living conditions	-1,1,2	-0.9	-0.9
72. Pica (consumption of nonnutritive substances)	-1,1,2	-0.9	-0.9
73. Troublesome sexual behavior	-1,1,2	-0.9	-0.9

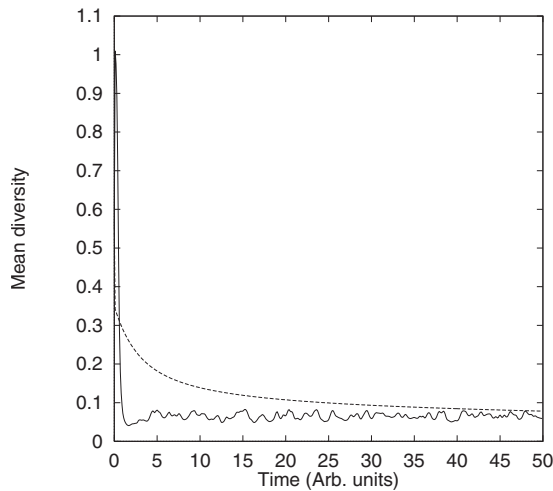


FIG. 1. Mean diversity σ as a function of dimensionless time. Solid line: Results using Eq. (7). Dashed line: Results using Eq. (14).

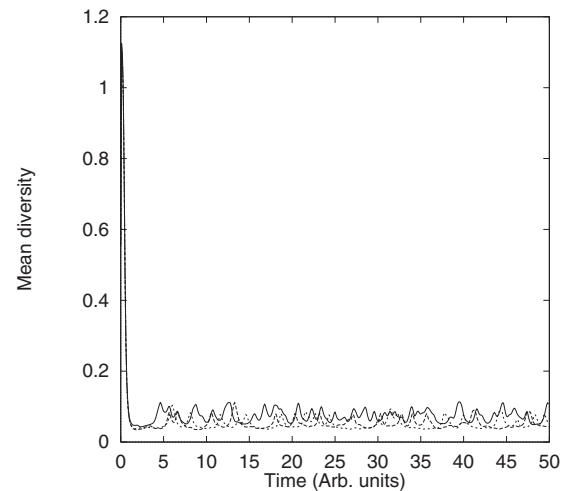


FIG. 2. Mean diversity σ as a function of dimensionless time for results for the three sets of data (indicated by solid, dashed, and dotted lines, respectively) provided by Otsu City using Eq. (7) with stubborn vectors.

more than three groups that consist of fewer oscillators [15]. For the feature extraction of the aging process from the care-needs-certification data, $\alpha=0.7$ may be the most suitable value in that it yields major features with high medical plausibility. It is an open question, however, whether there is a universal procedure for determining the optimal coarse-graining level that is applicable to every application of data synchronization.

The coupling constant K should be set so as to satisfy the necessary condition for achieving the fixed points of the governing equations, as was naively done in the numerical experiments. However, determining the values of K that ensure the stability of partial synchronization in a finite network of coupled phase oscillators is a subtle and difficult problem. Recently, De Smet and Aeyels considered this problem and derived a sufficient condition for achieving partially synchronous states of the finite Kuramoto-Sakaguchi model [16]. Although their argument might be applicable for the solutions of Eq. (7), its straightforward application to the solutions of Eq. (14) may be difficult because of the substantial modification of the finite Kuramoto-Sakaguchi model in the construction of Eq. (14). Thus, the stability of the partially synchronous solutions of our governing equations is another open problem.

In the first numerical experiment using the nationwide data, essentially the same three major patterns for elderly people needing nursing care were extracted whether using the dynamics of Eq. (7) or Eq. (14). Hence, we labeled these patterns as classes 1, 2, and 3. The main feature of class 1 is of functionally impaired legs that result in hindered movement when walking or using the legs. Class 3 features the progressive impairment of the legs in parallel with a noticeable deterioration in short-term memory and mental judgment. Class 2, meanwhile, falls within the process of worsening health from class 1 to class 3. The facts that the same patterns were obtained despite differences in dynamics and that data synchronization with the same order was achieved suggest that the patterns extracted by data synchronization are not an artifact peculiar to the dynamics used but rather may be the general features of the data group. The patterns in elderly people needing nursing care typified by classes 1, 2, and 3 are similar to the patterns in age-related functional impairments that have been recognized for some time. In this context, the results obtained from this experiment reflect reality.

In the second experiment using the data provided by Otsu City, class 1 was successfully reproduced, despite differences in the data targeted for analysis. Hence, we can conclude that

class 1 represents a major feature pattern of the aging process. In contrast, classes 2 and 3 were not reproduced as major patterns, despite using these classes as the stubborn vectors. Instead, a new major class labeled as class 4 emerged. The main feature of class 4 is the progressive impairment of the legs and deteriorating ability at daily living without a decrease in mental judgment that hinders social daily living. One possible interpretation of these experimental results is that classes 2 and 3 are particular feature patterns specific to the selected data sets. However, there is another possible interpretation, that class 4 could be a progressive version of class 1, and the nonappearance of classes 2 and 3 could be due to there being fewer elderly residents suffering from serious illness in the city. That is, these results may reflect the particular aspects of the aging process in Otsu City that are not in agreement with classes 2 and 3. This might be plausible, since the population ensemble from which the learning examples were randomly selected for the first experiment is much larger than that of the second experiment. Within the present work, it would be prudent to conclusively evaluate the generality of classes 2 and 3.

VI. CONCLUSION

In this study, we introduced collective synchronization in a data set, i.e., data synchronization, and evaluated a data mining method that induces a phase transition in a data set and extracts general features from sparse multivariate data. We demonstrated that data synchronization can reproduce the competitive learning rule for SOM when the governing equations are linearized about partially synchronized states. Many unresolved issues remain in this field including the link between the stability of partial synchronization and the reliability of extracted patterns, a universal procedure for determining the value of the coarse-graining parameter α that should be used in partial synchronization, and the testing of data synchronization as a valid data mining technique by applying it to diverse forms of multivariate data. We plan to continue our research on data synchronization with the aim of resolving these issues.

ACKNOWLEDGMENTS

The authors would like to extend their deep appreciation to Sadanori Higashino and Hitoshi Taniguchi for their invaluable advice and technical support throughout the course of this research. Part of this research was supported by a grant from the Ministry of Health, Labour and Welfare. The authors also thank Otsu City for their kind cooperation.

-
- [1] T. Kohonen, *Biol. Cybern.* **43**, 59 (1982).
 [2] T. Kohonen, *Proc. IEEE* **78**, 1464 (1990).
 [3] T. Miyano and T. Tsutsui, *Phys. Rev. Lett.* **98**, 024102 (2007).
 [4] Y. Kuramoto, *Chemical Oscillations, Waves, and Turbulence* (Springer, New York, 1984).
 [5] S. H. Strogatz, *Physica D* **143**, 1 (2000).

- [6] R. E. Mirollo and S. H. Strogatz, *Physica D* **205**, 249 (2005).
 [7] J. A. Acebrón, L. L. Bonilla, C. J. P. Vicente, F. Rotort, and R. Spigler, *Rev. Mod. Phys.* **77**, 137 (2005).
 [8] L. A. Aguirre, E. C. Furtado, and L. A. B. Tôrres, *Phys. Rev. E* **74**, 066203 (2006).
 [9] R. Brown, N. F. Rulkov, and E. R. Tracy, *Phys. Rev. E* **49**,

- 3784 (1994).
- [10] L. A. B. Tôrres, *Physica D* **228**, 31 (2007).
- [11] T. Tsutsui and N. Muramatsu, *J. Am. Geriatr. Soc.* **53**, 522 (2005).
- [12] J. C. Campbell and N. Ikegami, *Health Aff* **19**, 26 (2000).
- [13] T. Miyano, T. Tsutsui, Y. Seki, S. Higashino, and H. Taniguchi, *IEEE Trans. Inf. Technol. Biomed.* **9**, 502 (2005).
- [14] Currently, there are eight care classes used to certify the health status of an elderly person in need of care.
- [15] T. Miyano and T. Tsutsui, *Proceedings of 6th International Special Topic Conference on Information Technology Application in Biomedicine 2007* (IEEE, Tokyo, 2007), p. 153.
- [16] F. De Smet and D. Aeyels, *Physica D* **234**, 81 (2007).